

A Generative Model for Brain Tumor Segmentation in Multi-Modal Images

David Bourque
McGill University
Id: 260670624

david.bourque@mail.mcgill.ca

Abstract

For this project I chose to attempt to replicate a paper by Bjoern H. Menze, Koen Van Leemput et al. [7]. In the paper they describe how to build and train a generative model for brain tumor segmentation of multi-modal images. The method is fully automatic, requiring only the images and a probabilistic tissue map, which is assumed to be known.

1. Introduction

MRI (magnetic resonance imaging) is a common imaging method for the study of brain tumors. Currently, images are As such there is a need to be able to automatically identify tumors in the scans of a subject. Furthermore modern MRI machines can produce several different types of scans, for example FLAIR, which suppress' cerebrospinal fluid effects on an image, and often images for a patient are available for several different modalities. Standard multi-modal segmentation's (at the time the article was written) find a single tumor region for all modalities, however tumor areas may be delineated differently in each modality. Therefore, delineating tumor areas separately in each modality would be ideal for any further analysis. To that end the authors presented a generative model for multi-modal tumor segmentation that allows for a different segmentation in each modality. For comparison the authors also segmented the images using an EM segmentation similar to [8]. The authors showed a significant improvement in Dice scores for all modalities they tested (T1, T1 gad, T2 and Flair). For my project I attempted to implement their algorithm and perform segmentation on a data set of multi modal images with glioma's. The paper is outlined as follows: in section 2 I describe the theory behind their algorithm, section 3 describes the data sets I used, section 4 describes my implementation, finally, section 5 I discuss my results (or lack thereof).

2. Theory

Descriptive models attempt to directly predict the desired quantity $p(y|x)$ (y is the presence of tumors in this case), and so, do not consider spatial priors. To do so they generally require a lot of training data. They are also generally limited to the modalities present in the training data. Generative models model the joint probability distribution $p(x, y)$ and use Bayes theorem to try and compute $p(y|x)$. Using Bayes theorem, in this instance, requires knowing the spatial prior for tumors, which can be difficult to compute. To solve this problem the authors model uses an EM like algorithm to derive the spatial prior (for a particular patient) for tumor tissue. The model also includes a spatial prior on healthy tissues. For their paper, and my project, $K = 3$ healthy tissue types were considered, white matter, gray matter and cerebrospinal fluid. See Fig. 1 for an illustration of the model. Since the algorithm trains and segments simultaneously on a given set of images it generalizes well to any set of modalities. The basic model, while it does consider voxels across channels, does not encode any other spatial information. Although the prior π_k does encourage smoothness as neighboring voxels will have similar probabilities. The authors propose an extension to include in α a Markov Random Field spatial prior. They also extend the model to include more tissue classes for tumors, so segment the tumor itself into tissue types, active and necrotic areas etc.. For my project I only implemented the basic model.

2.1. Model

The prior on the normal tissue state K is modeled with π_k , which is a spatial probability map, or atlas, for the 3 tissue types, and is assumed to be known. The atlas defines, for each voxel i , a probability of belonging to tissue class k :

$$p(k_i = k) = \pi_{ki} \quad (1)$$

The model also uses a latent atlas α , which is unknown and derived as part of the algorithm. The latent alpha parametrizes t , which is the probability of a tumor at voxel i . t takes values $\{0, 1\}$ and is modeled as a Bernoulli ran-

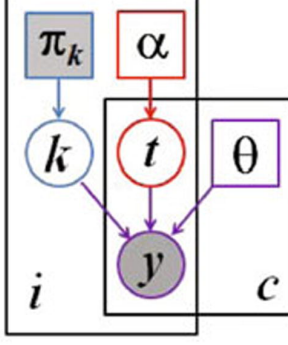


Figure 1. Graphical model from [7]. Only shaded values are known. π_k is the known prior for healthy tissue. \mathbf{y} are image observations

dom variable with probability α

$$p(t_i = 1) = \alpha_i \quad (2)$$

The values for π_k and α were shared across all channels.

Observations, \mathbf{y} , are generated by Gaussian intensity distributions. An intensity distribution parameter θ holds parameters μ_k^c and v_k^c for each of the C channels and K tissue classes, μ_{k+1}^c and v_{k+1}^c are added for each channel to represent the tumor class. For each voxel i the vector $\mathbf{y}_i = [y_i^1, \dots, y_i^C]$ represents the image observations across all C channels. Similarly the vector $\mathbf{t}_i = [t_i^1, \dots, t_i^C]$ represents the tumor state for all channels at voxel i . The authors state the joint probability:

$$p(\mathbf{y}_i, \mathbf{t}_i, k_i; \theta, \alpha_i) = p(\mathbf{y}_i | \mathbf{t}_i, k_i; \theta) \cdot p(\mathbf{t}_i; \alpha_i) \cdot p(k_i) \quad (3)$$

Equation 4 in [7](See also equations 1,2,3 in [7])

2.2. Maximum Likelihood and EM

The intended goal is to find optimal parameters $\{\tilde{\theta}, \tilde{\alpha}\}$, that maximize the likelihood of the observations $\mathbf{y}_1, \dots, \mathbf{y}_N$, where N is the number of voxels. To do so, an EM process is performed, first optimizing α , then optimizing θ . Iterations are continued until the maximum likelihood converges. For this they define two functions, one for the probability of any of the 2^C possible configurations of \mathbf{t}_i :

$$q_i(\mathbf{t}_i) \triangleq p(\mathbf{t}_i | k_i, \mathbf{y}_i; \theta, \alpha) \propto \sum_{k_i} p(\mathbf{y}_i | \mathbf{t}_i, k_i; \theta) \cdot p(\mathbf{t}_i; \alpha_i) \cdot p(k_i) \quad (4)$$

Equation 5 from [7](See also equations 1,2,3 in [7])

The authors define a similar function $w_{ik}(\mathbf{t}_i)$ for $p(k_i | \mathbf{t}_i, \mathbf{y}_i; \theta, \alpha)$, for the posterior probability of k_i . These equations are used in the update steps for α and θ (See unnumbered equations after equation 5 in [7]).

2.3. Tumor Segmentation

A voxel i in channel c is assigned a value 1 if $p(t_i^c | \mathbf{y}_i; \tilde{\theta}, \tilde{\alpha}) > 0.5$ (See equation 6 in [7])

3. Data

In [7] the authors used an unspecified data set containing 25 sets of patient images. Each set contained T_1 , T_2 , FLAIR, and post-Gadolinium T_1 images, with tumors manually segmented. For my project I chose to use the BRATS 2013 data set [6][4]. I chose this as it is a publicly available data set, containing real images (some other sets contain synthetic images) with manual segmentation's. Also, Menze, the first author of [7] is also the first author of [6], so they may (although I am guessing) contain some of the same images, although it is not really important. From the data set I chose the 20 sets of images for patients with high grade glioma, with four modalities, T_1 , T_2 , T_{1c} , and FLAIR. In each set all images had already been registered to the T_1 image, and each set contained a ground truth segmentation. The probabilistic spatial prior used was generated from the probability maps from the MNI-ICBM 152 non-linear atlas, version 2009 [3][2]

4. Experiment

Before segmentation some preprocessing was necessary. The spatial probability maps were registered onto the T_1 image for each set using the advanced normalization tool (ANTs). The registered maps were used to make the spatial prior π_k . An initial segmentation was also performed, on the T_1 images, to initialize variables θ and α . In [7] the authors state they used a freely available implementation of the algorithm in [5], however I was unable to find it. Regardless they segmented the images into 3 healthy classes and an outlier. The outlier was defined as voxels with intensity more than 3 standard deviations away from the mean of any of the 3 tissue classes. For this I again used ANTs, (via Atrapos [1]) to segment the images into 3 tissue classes. The mean and standard deviation were calculated for each class, and I further segmented the image by adding the outlier class. Because the segmentation by ANTs was unlabeled, I compared the segmentation's to the spatial prior, which was labeled. The initial segmentation that best matched the spatial prior for tissue k was labeled with class k , thus the labels for the atlas π_k matched the derived labels for the segmentation. The best match was taken as the class k that had the highest mean probability for all voxels in a particular segmentation.

Initial μ_k^c and v_k^c were set based on the segmentation of the healthy tissues, μ_{k+1}^c and v_{k+1}^c were set with the mean and variance of the outlier class. The latent atlas α was initialized with segmentation of the outlier class, voxels that

were part of the outlier class were set to $\alpha_i = 0.7$, all other α_i were set to 0.3.

My code was written in python2.7, using jupyter. SimpleITK was used to load and handle images.

5. Discussion

5.1. results

Unfortunately, at the time of this writing, I was unable to produce results. I had difficulty with ANTs installation which delayed the project. Mostly, however, it is due to the very large run times for my code. Working with full images, updating α

$$\alpha_i \leftarrow \sum_{t_i} q_i(t_i) \left(\frac{1}{C} \text{sum}_c t_i^c \right) \quad (5)$$

Unnumbered equation, below equation 5 in [7]

takes approximately one hour, with the operation vectorized and only those α_i that are not part of the background updated. Updating θ takes significantly longer.

$$\mu_k^c \leftarrow \frac{\sum_i \sum_{t_i} q_i(t_i) w_{ik}(t_i) (1 - t_i^c) y_i^c}{\sum_i \sum_{t_i} q_i(t_i) w_{ik}(t_i) (1 - t_i^c)} \quad (6)$$

Unnumbered equation, under equation 5 in [7]

Similar update are required for v_k^c , μ_{k+1}^c and v_{k+1}^c , with $C = 4$ and $K = 3$ the second step of the EM algorithm requires 16 updates. For the full images I halted it after the program had run for approximately 6 hours and only the first μ_1^1 had been updated. I then shrank the images, with SimpleITK, to $\frac{1}{3}$ the size in every dimension. which reduced the total number of voxels from 6 082 560 to 221 328. At this point I was more going for proof of functionality, rather than good results, as such a large decrease in resolution would make any segmentation fairly inaccurate. While running faster the algorithm still took approximately 14 hours to perform one iteration of EM, in [7] they state it took 10-15 iterations on average to converge, meaning running until convergence would be unfeasible. Much to my dismay this means I can only claim that my code does not crash. I have since changed the code to operate in 2D, on a single slice from each modality. From manual inspection of the ground truth I selected a depth in the horizontal plane that contains a large amount of tumor tissue. I then sliced each modality, and the initial segmentation at this same level. The algorithm is currently running, much faster, although i still project time to completion for 10 iterations to be approximately 20 hours. I could again reduce the size of the images, and take a slice, however, considering this project is already overdue I am forced to submit what I have.

References

- [1] B. B. Avants, N. J. Tustison, J. Wu, P. A. Cook, and J. C. Gee. An open source multivariate framework for n-tissue segmentation with evaluation on public data. *Neuroinformatics*, 9(4):381–400, 2011.
- [2] V. Fonov, A. Evans, R. McKinstry, C. Almli, and D. Collins. Unbiased nonlinear average age-appropriate brain templates from birth to adulthood. *NeuroImage*, 47, Supplement 1:S102 –, 2009. Organization for Human Brain Mapping 2009 Annual Meeting.
- [3] V. Fonov, A. C. Evans, K. Botteron, C. R. Almli, R. C. McKinstry, and D. L. Collins. Unbiased average age-appropriate atlases for pediatric studies. *NeuroImage*, 54(1):313 – 327, 2011.
- [4] M. Kistler, S. Bonaretti, M. Pfahrer, R. Niklaus, and P. Büchler. The virtual skeleton database: An open access repository for biomedical research and collaboration. *J Med Internet Res*, 15(11):e245, Nov 2013.
- [5] K. V. Leemput, F. Maes, D. Vandermeulen, and P. Suetens. Automated model-based tissue classification of mr images of the brain. *IEEE Transactions on Medical Imaging*, 18(10):897–908, Oct 1999.
- [6] B. Menze, A. Jakab, S. Bauer, J. Kalpathy-Cramer, K. Farahani, J. Kirby, Y. Burren, N. Porz, J. Slotboom, R. Wiest, L. Lanczi, E. Gerstner, M.-A. Weber, T. Arbel, B. Avants, N. Ayache, P. Buendia, L. Collins, N. Cordier, J. Corso, A. Criminisi, T. Das, H. Delingette, C. Demiralp, C. Durst, M. Dojat, S. Doyle, J. Festa, F. Forbes, E. Geremia, B. Glocker, P. Golland, X. Guo, A. Hamamci, K. Iftekhariuddin, R. Jena, N. John, E. Konukoglu, D. Lashkari, J. Antonio Mariz, R. Meier, S. Pereira, D. Precup, S. J. Price, T. Riklin-Raviv, S. Reza, M. Ryan, L. Schwartz, H.-C. Shin, J. Shotton, C. Silva, N. Sousa, N. Subbanna, G. Szekely, T. Taylor, O. Thomas, N. Tustison, G. Unal, F. Vasseur, M. Wintermark, D. Hye Ye, L. Zhao, B. Zhao, D. Zikic, M. Prastawa, M. Reyes, and K. Van Leemput. The Multimodal Brain Tumor Image Segmentation Benchmark (BRATS). *IEEE Transactions on Medical Imaging*, page 33, 2014.
- [7] B. H. Menze, K. Leemput, D. Lashkari, M.-A. Weber, N. Ayache, and P. Golland. *Medical Image Computing and Computer-Assisted Intervention – MICCAI 2010: 13th International Conference, Beijing, China, September 20-24, 2010, Proceedings, Part II*, chapter A Generative Model for Brain Tumor Segmentation in Multi-Modal Images, pages 151–159. Springer Berlin Heidelberg, Berlin, Heidelberg, 2010.
- [8] M. Prastawa, E. Bullitt, S. Ho, and G. Gerig. A brain tumor segmentation framework based on outlier detection. *Medical Image Analysis*, 8(3):275–283, 9 2004.

Brain tumor image data used in this work were obtained from the NCI-MICCAI 2013 Challenge on Multimodal Brain Tumor Segmentation (<http://martinos.org/ctim/miccai2013/index.html>) organized by K. Farahani, M. Reyes, B. Menze, E. Gerstner, J. Kirby and J. Kalpathy-Cramer. The challenge database contains fully anonymized images from the following institutions: ETH Zurich, University of Bern, University of Debrecen, and University of

Utah and publicly available images from the Cancer Imaging Archive (TCIA).